Ultrasound in Med. & Biol., Vol. 43, No. 9, pp. 2045–2053, 2017
© 2017 World Federation for Ultrasound in Medicine & Biology
Printed in the USA. All rights reserved
0301-5629/$ - see front matter

http://dx.doi.org/10.1016/j.ultrasmedbio.2017.05.018

● *Original Contribution*

THREE-DIMENSIONAL ECHOCARDIOGRAPHY-DERIVED NON-INVASIVE RIGHT VENTRICULAR PRESSURE-VOLUME ANALYSIS

KUAN-CHIH HUANG,*† LIAN-YU LIN,‡ JUEY-JEN HWANG,‡ and LUNG-CHUN LIN‡

*National Taiwan University Hospital Jin-Shan Branch, New Taipei City, Taiwan; †Graduate Institute of Clinical Medicine, National Taiwan University College of Medicine, Taipei, Taiwan; and ‡Division of Cardiology, Department of Internal Medicine, National Taiwan University Hospital, Taipei, Taiwan

(*Received* 26 *January* 2017; *revised* 13 *May* 2017; *in final form* 18 *May* 2017)

Abstract—In patients with pulmonary hypertension, repeated evaluations of right ventricular (RV) function are still required for clinical decision making, but the invasive nature of current pressure-volume analysis makes conducting regular follow-ups in a clinical setting infeasible. We enrolled 12 patients with pulmonary arterial hypertension (PAH) and 10 with pulmonary venous hypertension (PVH) May 2016–October 2016. All patients underwent a clinically indicated right heart catheterization (RHC), from which the yielded right ventricular pressure recordings were conjugated with RV volume by 3-D echocardiography to generate a pressure-volume loop. A continuous-wave Doppler envelope of tricuspid regurgitation was transformed into a pressure gradient recording by the simplified Bernoulli equation, and then a systolic pressure gradient-volume (PG-V) diagram was generated from similar methods. The area enclosed by the pressure-volume loop was calculated to represent semi-invasive right ventricular stroke work ($RVSW_{RHC}$). The area between the PG-V diagram and x-axis was calculated to estimate non-invasive RVSW ($RVSW_{echo}$). Patients with PAH have higher RV pressure, lower pulmonary arterial wedge pressure and larger RV volume that was contributed by the dilation of RV mid-cavity minor dimension. We found no significant difference of traditional parameters between these two groups, but RVSW values were significantly higher in PAH patients. The RVSW values of these two methods were *significantly* correlated by the equation $RVSW_{echo} = 0.8447\ RVSW_{RHC} + 129.38$ ($R^2 = 0.9151$, $p < 0.001$). The linearity remained satisfactory in both groups. We conclude that a PG-V diagram is a reliable method to estimate RVSW and to depict pathophysiological status. (E-mail: anniejou@ms28.hinet.net) **© 2017 World Federation for Ultrasound in Medicine & Biology.**

Key Words: **Pressure-volume loop, Pulmonary hypertension, Three-dimensional echocardiography.**

INTRODUCTION

In the mammalian cardiovascular system, the right ventricle (RV) performs the very first of the in-series double pumps. Its functioning reflects a composite result of fluid status, pulmonary vascular resistance and left heart function, and its failure to function properly is implicated in several cardiac diseases (Dandel et al. 2015; Gorcsan et al. 1996; Mohammed et al. 2014; Vachiéry et al. 2013). However, the parameters of RV function that can be measured non-invasively, such as right ventricular ejection fraction (RVEF), tricuspid annular plane systolic excursion (TAPSE), tricuspid regurgitation pressure gradient (TRPG), fractional area change, peak systolic longitudinal RV free wall strain, the RV index of myocardial performance and the load adaptation index, are considered to be only of modest predictive value in the prognosis of heart disease (Bleeker et al. 2006; Cameli et al. 2014; Guihaire et al. 2013; Ling et al. 2012). This is because the RV alters its shape continuously throughout its unique peristalsis-like contraction, but the above parameters only focus on static differences between the end-diastole and end-systole. As a result, the dynamic pumping process has been overlooked as has the individual contractive contribution made by each of the three parts of the RV, among which the infundibulum makes the last and longest contribution (Haddad et al. 2008).

The pressure-volume (PV) loop is the fundamental analytic tool of cardiac physiology. It is used to derive stroke work and elastance (Kass et al. 1986), which have played important roles in left ventricular (LV)

Address correspondence to: Lung-Chun Lin, Division of Cardiology, Department of Internal Medicine, National Taiwan University Hospital, No. 7, Chung-Shan South Road, Taipei 10002, Taiwan, R.O.C. E-mail: anniejou@ms28.hinet.net

evaluation beyond ejection fraction. A simultaneous high-quality recording of pressure and volume is the key for making use of the PV loop to analyze heart function. However, the complex geometry and abundant trabeculation of the right ventricle tend to hinder volumetric analysis. Geometric approximation of RV volume by two-dimensional echocardiography methods, such as fractional area change, totally overlook the contractive contribution of the infundibulum and cannot reflect the peristaltic bellows-like effect of RV contraction. A conductance catheter, being invasive in nature, makes conducting regular follow-ups in a clinical setting infeasible. Cardiac magnetic resonance imaging, the current gold standard for RV volume measurement, also requires an invasive technique to generate a PV loop (Kuehne 2004).

Echocardiography, the traditional tool of cardiac evaluation, has been widely used because of its good accessibility. Recently, multiple-beat reconstructed three-dimensional echocardiography (3-DE) and dedicated software for endocardial border tracking have brought volumetric analysis from theory into clinical practice. Not only does 3-DE show good consistency with cardiac magnetic resonance imaging in volume measurement (Medvedofsky et al. 2015), echocardiography also makes possible calculation of the pressure gradient, using the simplified Bernoulli equation. Because the diastolic pressure recording is in a low pulsatile pattern in the right heart (Ensing et al. 1994), the difference between its peak-to-peak pressure gradient and maximum pressure gradient diminishes to a negligible degree. As a result, we hypothesized that the tricuspid regurgitation pressure gradient (TRPG) recording calculated by spectral Doppler envelope tracing might have a similar curvilinear character to the right heart catheterization (RHC) pressure recording and should be applicable in estimating right ventricular stroke work (RVSW). The aim of this study is to examine the consistency between non-invasive RVSW derived from echocardiography ($RVSW_{echo}$) and semi-invasive RVSW yielded from RHC and 3-DE ($RVSW_{RHC}$) in terms of curvilinear character and stroke work values to provide a feasible method for clinical follow-ups.

MATERIALS AND METHODS

Patients

May 2016–October 2016 we enrolled twelve patients diagnosed with pulmonary arterial hypertension (PAH) and ten with pulmonary venous hypertension (PVH). Among the PAH patients, five were diagnosed with idiopathic pulmonary arterial hypertension (group 1) and seven were diagnosed with chronic thromboembolic pulmonary hypertension (group 4). The PVH patients all belonged to group 2 pulmonary hypertension. All of them underwent 3-DE, followed by a clinically indicated RHC. Informed consent was obtained and the institutional review board of National Taiwan University Hospital approved the collection protocol (201601071 RINC). Meeting the requirements for reimbursement of costs for PAH treatment and pre-operative evaluation for valvular heart disease were the only two indications for RHC in the present study. Patients with atrial fibrillation and other irregular heart beat arrhythmia were excluded because of the difficulty of performing the multiple-beat-reconstruction step of 3-DE in such patients.

Echocardiography

All echocardiographs were performed with the iE33 system equipped an X5-1 transducer (Philips Medical Systems, Andover, MA, USA). Two-dimensional RV parameters were measured as suggested by Rudski et al. (2010). Right ventricle 3-DE data sets were obtained from RV four chamber views adjusted to avoid a pulmonary shielding effect on the RV outflow tract (Lang et al. 2012). Continuous-wave Doppler recordings of the maximal tricuspid regurgitation (TR) envelope were obtained systematically from lower left parasternal long-axis RV inlet views, parasternal short axis views, apical long axis RV inlet views, apical four chamber views and subcostal transducer positions. The chosen TR envelope should have the highest velocity, the cleanest signal without envelope truncation in the whole spectral Doppler recording. When remarkable beat-to-beat variation occurred during respiration, TR velocity was acquired at the end-expiration, which is the most often used time frame for multiple-beat reconstruction of 3-DE. TR velocity recordings were transformed into TRPG tracings through the simplified Bernoulli's equation: $TRPG = 4 \times Vel^2$ (Vel = peak velocity of tricuspid regurgitation, m/s; TRPG calculated in mmHg). RV volumes and right ejection fraction (RVEF) were obtained from 3-D data sets that were analyzed offline with a module for RV volumetric analyses (4D RV-Function 2.0, Image-Arena v. 4.6, TOMTEC Imaging Systems, Unterschleissheim, Germany).

Pressure recording

A fluid-filled catheter was delivered into the apex of the right ventricle under fluoroscopy and RV pressure was measured with a calibrated pressure transducer. Catheterization pressure curves were recorded along with electrocardiography (ECG) signals using a commercially available hemodynamic recording system (Axiom Sensis XP Cath Lab Monitoring, Siemens Healthcare, Munich, Germany).

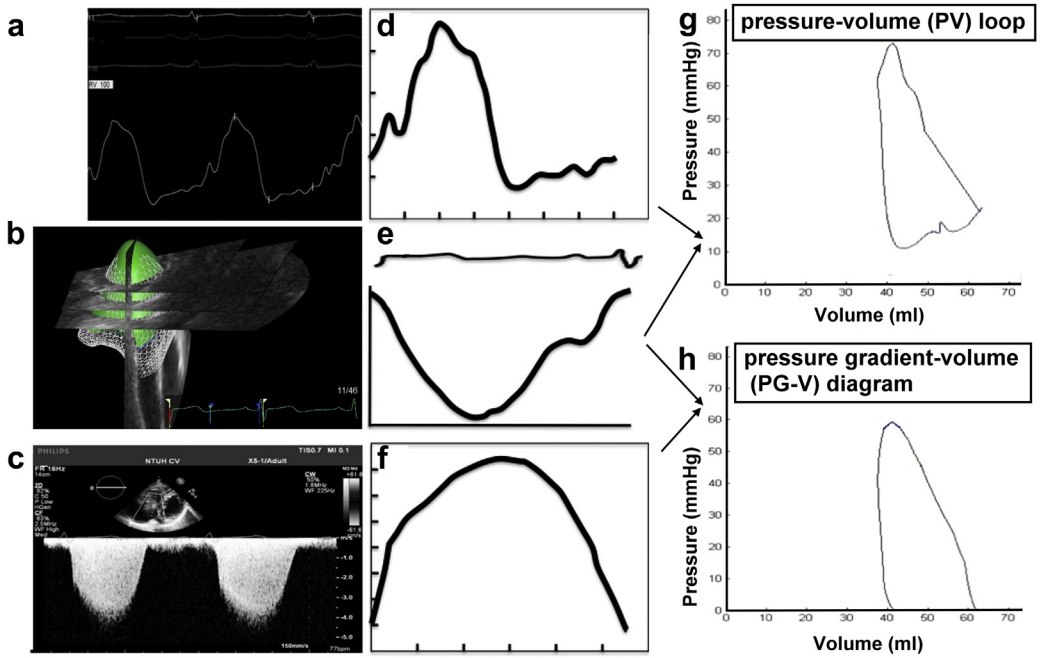

Fig. 1. Methods to generate the PV loop and PG-V diagram. (a) Right ventricular pressure was invasively measured by the right heart catheterization with a (d) digitalized conversion. The pressure gradient was non-invasively estimated by the (c) spectral Doppler of tricuspid regurgitation with (f) envelope extraction to be transformed through the simplified Bernoulli's equation. (b)Three-dimensional echocardiographic data sets provided the (e) common information of volumetric alteration in a cardiac cycle. Conjugation of pressure and volume data based on the cycle length was performed using the MATLAB software (MathWorks) to generate the (g) PV loop and (h) PG-V diagram. PV = pressure-volume; PG-V = pressure gradient-volume.

Plotting of the PV relationships

We plotted the pressure volume relationships (Fig. 1). A clear ECG signal should be acquired simultaneously along with each TR envelope, 3-DE RV data set and RHC pressure recording. Hemodynamic and volumetric data were resampled within the chosen R-R interval as one cardiac cycle to replot the PV loop and the systolic pressure gradient-volume (PG-V) diagram. Because of the 8–90 ms delay inherent in the fluid-filled pressure measurement system (Ensing et al. 1994), the pressure recording could not be extracted as the segment right under selected R-R interval. Instead, the extracted pressure recording should be started from the end-diastolic point, which is decided by the hemodynamic report system. The cycle length of the selected beat then determined the end of the extraction. This method is to prevent distortion of the yielded PV loop from an unnoticed phase shift. Although the phase shift might be negligible under the sonic speed conditions of the echo-derived PG-V diagram construction, the spatial resolution of the diastolic tricuspid inflow spectral envelopes is compromised under the macro-scale of the high TR velocity construction. On the other hand, the peak tricuspid inflow velocity is usually 40–60 cm/s (*i.e.,* pressure gradient of about 1 mmHg) (Rudski et al. 2010), and was arbitrarily omitted during the stroke work calculations. As a result, we only used the TR envelope for constructing the non-invasive PG-V diagram. The pressure-volume area of the PV loop was used to represent the RVSW; while for the PG-V diagram, the RVSW was approximated by the area under the curve. Figure plotting, measurement of stroke work and analysis of curve characteristics were performed with the MATLAB software program (MATLAB starter application R2009 a, MathWorks, Inc., Natick, MA, USA). Our method yielded a non-invasive PG-V diagram within 1 h, including image acquisition, offline volumetric analysis and MATLAB management.

Statistical analysis

Categorical variables were presented as numbers and percentages and were compared through a χ^2 test or Fisher exact test. Continuous variables were expressed as the mean ± standard deviation, and were compared using Student *t* test. A receiver operating characteristics curve was constructed to determine the optimal cut-off of chosen variables, as well as to make a comparison of predictions in terms of the area under the curve. Logistic regression was performed and the *p*-values of the Wald χ^2 statistics were used to rank the predictors. The similarity

between two curves was calculated on the basis of the MATLAB corrcoef function (MathWorks, Inc.). All statistical analyses were performed using SPSS Statistics for Windows (v. 17.0, IBM SPSS, Inc., Chicago, IL, USA). All reported p-values were 2-tailed, and p values < 0.05 were considered statistically significant.

RESULTS

The RHC data, parameters of echocardiography, and calculated $RVSW_{echo}$ and $RVSW_{RHC}$ values are listed in Table 1. Noninvasive PG-V diagrams and semi-invasive PV loops for all the patients are plotted in Figure 2 (a,b),

Table 1. Clinical characteristics and measurements*

	PAH (n = 12)	PVH (n = 10)	p Value
Male	4 (33.3)	4 (40)	0.760
Age (y)	56.7 ± 16.1	57.5 ± 12.5	0.895
BSA (m^2)	1.60 ± 0.25	1.56 ± 0.22	0.742
HR (bpm)	72.3 ± 10.1	76.2 ± 18.0	0.548
Right heart catheterization			
PASP (mmHg)	81.1 ± 21.2	53.8 ± 13.9	0.002
PADP (mmHg)	29.9 ± 6.3	21.6 ± 5.3	0.004
Mean PAP (mmHg)	47.6 ± 11.5	34.3 ± 8.31	0.007
Mean RAP (mmHg)	9.2 ± 3.5	6.0 ± 2.5	0.027
RVSP (mmHg)	81.3 ± 20.8	51.4 ± 14.7	0.001
PAWP (mmHg)	12.8 ± 3.7	23.1 ± 5.3	<0.001
Echocardiography			
TRPG (mmHg)	73.9 ± 21.1	49.2 ± 15.3	0.006
RVEDV (mL)	97.2 ± 34.8	72.5 ± 18.8	0.059
RVESV (mL)	62.2 ± 27.0	42.6 ± 14.0	0.043
RVSV (mL)	35.1 ± 10.2	29.9 ± 6.5	0.187
RVEF (%)	38.0 ± 11.0	42.2 ± 6.8	0.311
TAPSE (mm)	15.1 ± 2.9	15.9 ± 2.4	0.478
FAC (%)	36.4 ± 0.9	41.3 ± 9.1	0.219
RVLSfw (%)	17.5 ± 6.7	22.4 ± 6.0	0.089
RVD1 (mm)	28.9 ± 8.4	26.9 ± 5.3	0.520
RVD2 (mm)	38.0 ± 7.5	29.5 ± 5.9	0.008
RVD3 (mm)	76.6 ± 7.4	76.9 ± 10.6	0.925
$RVSW_{RHC}$ (mmHg × mL)	1533.3 ± 696.9	914.5 ± 313.3	0.014
$RVSWI_{RHC}$ (mmHg × mL/m^2)	984.3 ± 459.3	586.0 ± 191.5	0.015
$RVSW_{echo}$ (mmHg × mL)	1418.6 ± 618.9	909.1 ± 307.9	0.028
$RVSWI_{echo}$ (mmHg × mL/m^2)	915.0 ± 430.0	580.6 ± 180.0	0.027

PAH = pulmonary arterial hypertension; PVH = pulmonary venous hypertension; BSA = body surface area; HR = heart rate; PASP = pulmonary arterial systolic pressure; PADP = pulmonary arterial diastolic pressure; PAP = pulmonary arterial pressure; RAP = right atrial pressure; RVSP = right ventricular systolic pressure; PAWP = pulmonary arterial wedge pressure; TRPG = tricuspid regurgitation pressure gradient; RVEDV = right ventricular end-diastolic volume; RVESV = right ventricular end-systolic volume; RVSV = right ventricular stroke volume; RVEF = right ventricular ejection fraction; TAPSE = tricuspid annular plane systolic excursion; FAC = fractional area change; RVLSfw = peak systolic longitudinal RV free wall strain; RVD1 = RV basal dimension; RVD2 = RV mid cavity minor dimension; RVD3 = RV longitudinal dimension; $RVSW_{RHC}$ =right ventricular stroke work by right heart catheterization; $RVSW_{echo}$ = right ventricular stroke work by echocardiography; RVSWI = right ventricular stroke work index.

* Values are mean ± SD or n (%).

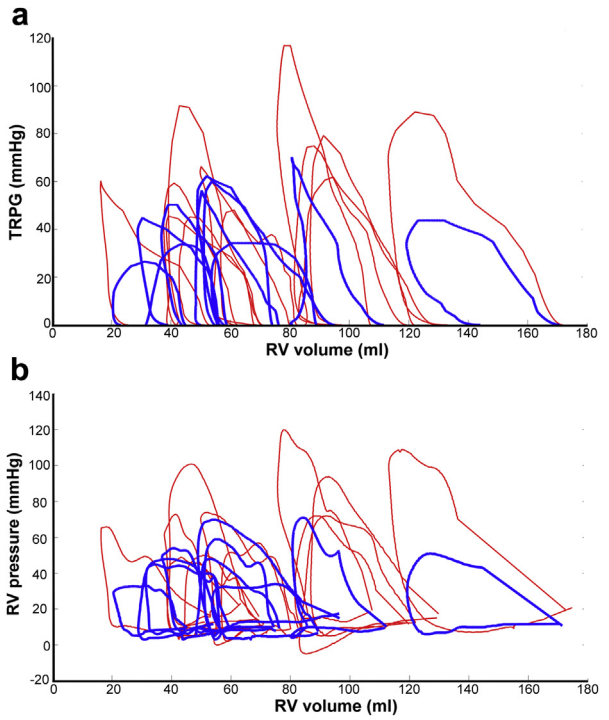

Fig. 2. (a) PG-V diagrams and (b) pressure-volume loops of 22 patients. (*red* = pulmonary arterial hypertension; *blue* = pulmonary venous hypertension). PG-V = pressure gradient-volume; RV = right ventricle; TRPG = tricuspid regurgitation pressure gradient.

respectively. Patients with PAH have higher pressure in the right cardiac chambers than patients with PVH, which instead have higher pulmonary artery wedge pressure. Volumetric analyses revealed a trend of larger RV end-diastolic volume and a significantly larger RV end-systolic volume in patients with PAH, with the greatest contribution coming from dilation of the RV mid-cavity minor dimension (RVD2). In terms of pumping function, no differences were found in the RVEF, TAPSE, fractional area change and longitudinal RV free wall strain values between these two groups, but RVSW values were significantly higher in PAH patients. $RVSW_{echo}$ correlated with $RVSW_{RHC}$ (Fig. 3b) significantly by the following equation:

$$RVSW_{echo} = 0.8447 RVSW_{RHC} + 129.38; \quad R^2 = 0.9151,\ p<0.001 \tag{1}$$

The similarity between systolic curves of non-invasive pressure gradient estimations and RHC pressure recordings was analyzed and the R-values ranged 0.325–0.995 (mean = 0.875, standard deviation = 0.172). To find out the non-invasive determinants hindering the similarity, we analyzed all the echo-derived parameters by way of stepwise multi-variable linear regression. TRPG was the only significant determinant of positive

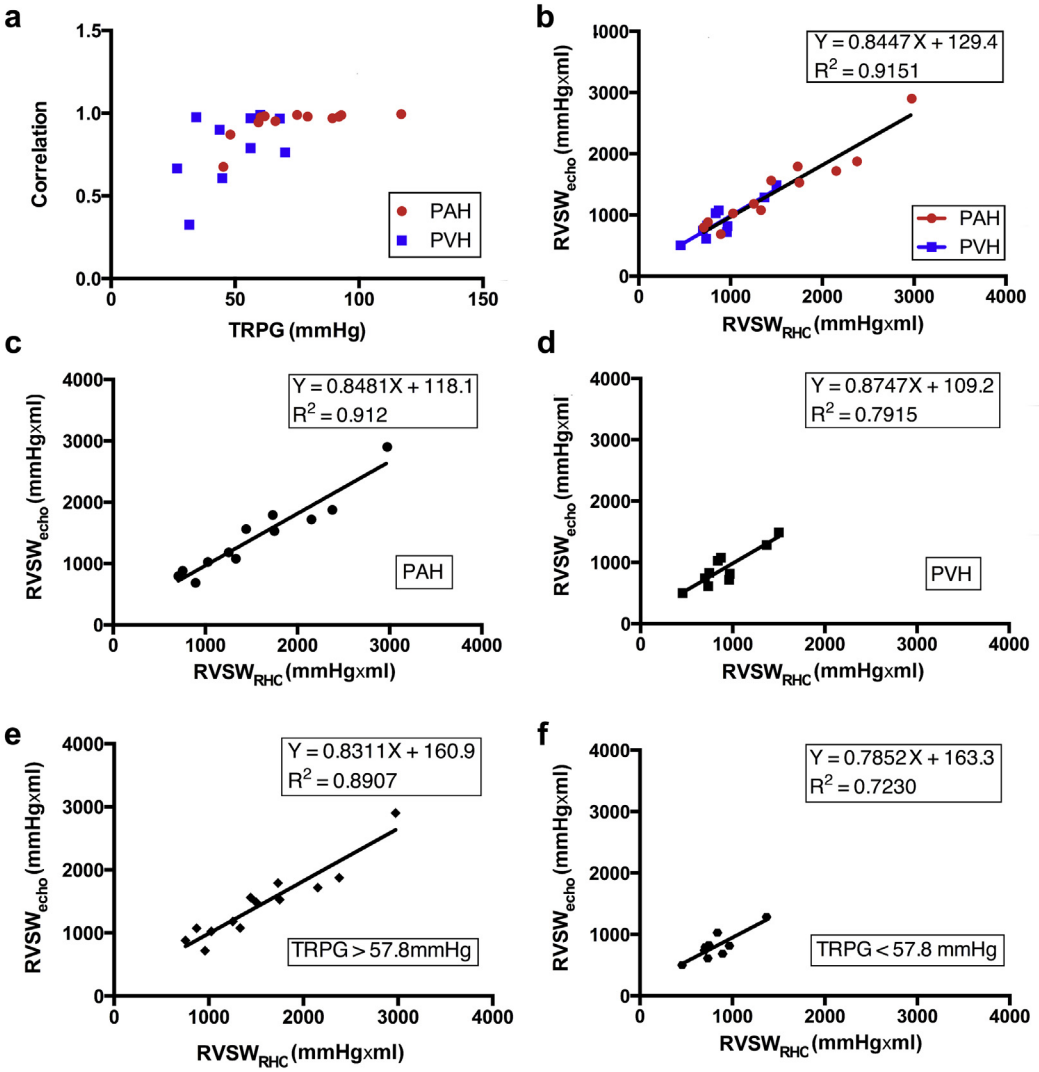

Fig. 3. Correlation of $RVSW_{echo}$ and $RVSW_{RHC}$. (a) Scatterplot of the correlation coefficient of two methods of pressure measurement versus TRPG. *Red* represents patients with PAH and *blue* represent patients with PVH. (b) Correlations of non-invasive RVSW ($RVSW_{echo}$) and invasive RVSW ($RVSW_{RHC}$) are shown for all 22 patients; (c) PAH; (d) PVH; (e) TRPG above 57.8 mmHg; and (f) TRPG under 57.8 mmHg. $RVSW_{echo}$ = right ventricular stroke work by echocardiography; $RVSW_{RHC}$ = right ventricular stroke work by right heart catheterization; TRPG = tricuspid regurgitation pressure gradient; PAH = pulmonary arterial hypertension; PVH = pulmonary venous hypertension.

correlation with similarity (β = 0.591; p = 0.004). Figure 3a shows the relationship between R-values of curves and TRPG and the R-values become more satisfactory as TRPG increases. We conducted receiver operating characteristics curve analysis of TRPG to predict an R-value greater than 0.850. The best cut-off point of TRPG was 57.8 mmHg (sensitivity 80.0%, specificity 85.7%; area under the curve = 0.862). Linearity of RVSW was retested for the different dichotomies, PAH versus PVH and low TRPG versus high TRPG. The R-square values obtained are 0.912 in PAH patients (n = 12, $p < 0.001$, Fig. 3c), 0.7915 in PVH patients (n = 10, $p < 0.001$, Fig. 3d); 0.8907 in TRPG above 57.8 mmHg (n = 13, $p < 0.001$, Fig. 3e) and 0.723 in TRPG under 57.8 mmHg (n = 9, p = 0.004, Fig. 3f).

RVSW and pulmonary artery wedge pressure were significantly correlated in PVH patients (R^2 = 0.547, p = 0.036) but not in PAH patients (R^2 = 0.254, p = 0.114).

DISCUSSION

The major finding of the present study is that RVSW can be estimated non-invasively by the method described to obtain a value that reliably correlates with that derived from a semi-invasive method. We also found no

significant differences between PAH and PVH patients with respect to traditional RV pumping parameters (*i.e.,* RVEF, TAPSE, fractional area change and longitudinal RV free wall strain), but the shapes of their RV were different, with more dilated RVD2 in PAH patients. This implies the pumping mechanism of RV is somehow different but unexplainable by most static parameters. The increase of RVD2 reflected either dysfunction or elongation of the septomarginal band and moderator band, implying the remodeling of the inlet and apex, respectively (Aguero et al. 2014).

Evolution of the dynamic substitution for static TRPG

Pulmonary artery systolic pressure estimated by TRPG is a traditional echo parameter for heart failure. This approach, using a velocity only at a single point in time and thus providing no curves comparable to RHC-measured pressure curves, should be modified because the feasibility of Doppler-derived RV pressure curves has been proven by more than 10 y of testing (Claessen et al. 2016; Currie et al. 1985; Ensing et al. 1994). Besides, in patients with PAH, pulmonary artery systolic pressure reaches a plateau soon after initial fluctuation and its interpretation is widely thought to be in need of contextualization with changes of stroke volume (Wright et al. 2016). On the other hand, in patients with left heart disease, the value of TRPG is variable because of load-dependence and, again, needs to be interpreted by simultaneous consideration of RV volume. In the past, RV volume measurement was hindered by complex geometry. The product of stroke volume of thermodilution method and RHC measured mean pulmonary arterial pressure was used as a substitute for RVSW and was applied for outcome prediction in several types of heart failure (Di Maria et al. 2015). Such methods of RVSW approximation were useful in the era lacking reliable pressure and volume recordings, but did not include the pulsatile factor of the pressure-volume relationship, which is more important in RV functioning (Chemla et al. 2013; Chesler et al. 2009). On the other hand, two-dimensional approximations of RVEF and RV stroke volume, such as fractional area change and velocity time integrals at right ventricular outflow tract, are neither recommended for clinical use nor as a standard reference in research (Rudski et al. 2010). However, these parameters are currently suggested to be approached by 3-DE, which allows direct assessments instead of geometric assumptions, resulting in more accurate and reproducible measurements (Lang et al. 2015).

Effects of RV shape on the performance of the conductance catheter

A conductance catheter, capable of simultaneously recording conductance volume and pressure tracing, formed a solid foundation for the development of LV physiology, but a much less solid foundation for the right-sided counterpart, as has been well studied (Dell'italia and Walsh 1988; McKay et al. 1984; Szwarc and Ball 1998). One of the most representative examples of this shaky foundation is the method of deriving RV elastance from inferior vena cava balloon occlusion, for which the assumption of a homogeneous electrical field was subject to routine violation caused by the abundant trabeculation that prevails in the right ventricle. Danton et al. (2003) have demonstrated a non-linear conductance-volume relationship, especially with changing loading conditions, which is a key component of the inferior vena cava occlusion method. In a cardiac magnetic resonance imaging study (Szwarc et al. 1995), curvilinearity of the gain factor was observed and the reliability of the Millar catheter (Millar Instruments, Inc., Chicago, IL, USA) derived end-systolic pressure-volume relationship was challenged. The thin RV wall does not offer enough insulation to parallel conductance. Although the RV wall might be thick enough in PAH patients, either progression of disease status or treatment could lead to a change of RV insulation. As a result, the data derived from this method might be grossly misleading when used in longitudinal follow-up.

Deduction from the PV loop to the PG-V diagram

As shown in Figure 3a, the TRPG should be high enough to neglect right atrial pulsation and allow the curvy character to be taken as the *de facto* RV pressure. We have to clarify again that the R-value is for the "curve similarity" rather than the value of recorded pressure and we do admit that the R-value is lower at the lower right ventricular pressure; this is because the difference of right ventricular pressure and TRPG (*i.e.,* right atrial pressure) would become more significant at lower TRPG. However, in the present study, the consistency of RVSW remained satisfactory even at a low level of TRPG. We proposed the following assumption: $RVSW_{RHC}$ is the RV pumping work measured in the inertial reference frame of atmosphere (Fig. 4, *blue area*), and the $RVSW_{echo}$ is the same physical quantity just measured in the non-inertial reference frame of a pulsatile right atrial pressure (Fig. 4, *yellow and green areas*).

$$\text{That is, } \textit{Blue Area} = \textit{Yellow Area} + \textit{Green Area}$$

Usually, the mean pressure of tricuspid inflow is less than 2 mmHg (Rudski et al. 2010). Average RV stroke volume was around 30 mL in this study (Table 1). As a result, the value of the *green area* in Figure 4 would be less than 60 mmHg × mL, which should be negligible during estimation of $RVSW_{echo}$.

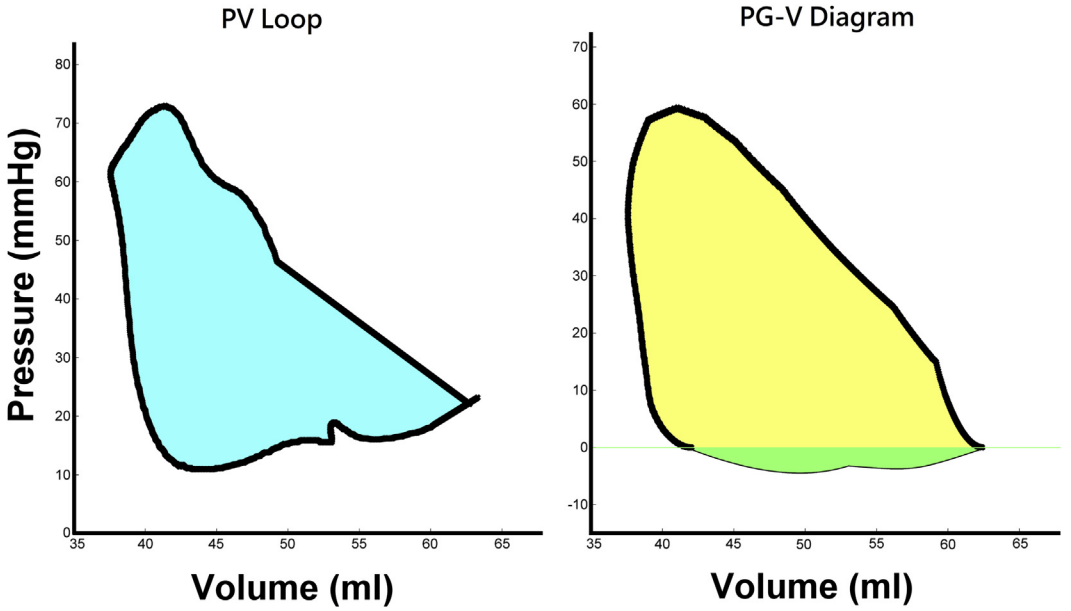

Fig. 4. Comparison of right ventricular stroke work (RVSW) estimation from pressure-volume (PV) loop and pressure gradient-volume (PG-V) diagram. Traditional area used for calculation of RVSW in PV loop analysis (*blue*). The area between the PG-V diagram and x-axis was used to estimate RVSW in the present study (*yellow*). An artificially illustrated representation of the negative work of right ventricle on right atrium during diastole (*green*). RVSW = right ventricular stroke work; PV = pressure volume; PG-V = pressure gradient-volume.

The above equation could be simplified as:

$$Blue\ Area = Yellow\ Area$$

And we have empirically proven the equation with these patients who have pulmonary hypertension.

Consideration of the PG-V diagram beyond RVSW

The idea of phenotyping (Ryo et al. 2015; Shah et al. 2015) of different cardiac diseases has been proposed recently in the field of heart failure with a preserved ejection fraction. Many non-invasive LV parameters, especially that from deformational imaging, have been included, but the right-sided parameters have not been widely adopted because of the inherently invasive nature. Peak tricuspid regurgitation velocity is the only right-sided variable that has been suggested by the American Society of Echocardiography guidelines to assess LV diastolic function (Nagueh et al. 2016). On the other hand, repeated studies for clinical decision making are required in patients who have PAH. Figure 5 contains the PV loops and PG-V diagrams of seven of the PAH patients (selected to avoid an overcrowded illustration). We found that even though some patients have similar RVSW values, as a cross-sectional group, they may actually have different disease statuses as implied by their location on the map of the PG-V diagram distribution. Such a phenomenon was less obvious in PVH patients (Fig. 2, *blue*), who were medically considered to have a similar preoperative status. As a result, the shape and distribution of PG-V diagram might also be applied for phenotyping in patients of pulmonary hypertension.

Study limitations

A potential limitation of this study is that the most decisive inclusion criterion was a clinically indicated RHC, which was one of the criteria to qualify for

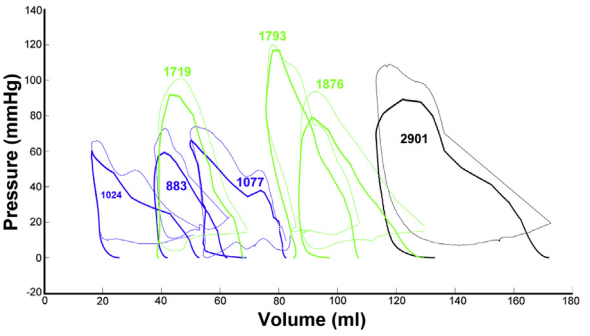

Fig. 5. Example of phenotyping on the basis of the concept of the PV relationship. Only 7 of the 12 pulmonary arterial hypertension patients were chosen (*to avoid an overcrowded illustration*). Even with similar RVSW values, the shape and location of the area representing the PV relationship on the PG-V diagrams/PV loops can help in evaluation of disease status. We set 3 colors to separate those 7 patients into 3 levels of RVSW. *Thin lines* indicate PV loops; *thick lines* indicate PG-V diagrams; *numbers* are values of RVSW in mmHg × mL. PV = pressure volume; RVSW right ventricular stroke work; PV-G = pressure gradient-volume.

reimbursement of fees paid for PAH medication or preoperative evaluation. As a result, the consistency of RVSW was not tested in those of end-stage heart disease or other critical illness who did not meet the qualifications to receive RHC. However, the major contribution of inconsistency resides in the diastolic pressure pulsation and the phase shift of pressure and volume recordings. The former becomes non-pulsatile in severe diastolic failure and the latter did not exist when the pressure and volume data source came from a single modality (*i.e.,* ultrasound). Another limitation of this technique is the lack of an absolute right atrial pressure recording and thus of a measurement of maximal RV elastance, which is considered a reliable index of RV contractility but cannot be obtained from our PG-V diagram. The final and also the most important limitation is the lack of comparison with a true gold standard (*i.e.,* conductance catheter) and the semi-invasive pressure volume loop for comparison is also a surrogate value. As mentioned earlier in this report, the conductance catheters also have limitations of their use in RV, but the volumetric analysis of RV by 3-DE is validated rather than calibrated by cardiac magnetic resonance imaging.

CONCLUSIONS

To the best of our knowledge, the present study is the first attempt to estimate RVSW non-invasively on the basis of the concept of the PV loop. We have shown that the measurement of RVSW can be achieved non-invasively in patients with pulmonary arterial and venous hypertension with practically no geometric approximation necessary. Although further validation with longitudinal data in clinical practice is needed, this non-invasive RVSW estimation should become an important addition to the repertoire of techniques used in the evaluation and management of pulmonary hypertension in the future.

Acknowledgments—The authors have no conflicts of interest to disclose related to the contents of this paper.

REFERENCES

Aguero J, Ishikawa K, Hadri L, Santos-Gallego C, Fish K, Hammoudi N, Chaanine A, Torquato S, Naim C, Ibanez B, Pereda D, García-Alvarez A, Fuster V, Sengupta PP, Leopold JA, Hajjar RJ. Characterization of right ventricular remodeling and failure in a chronic pulmonary hypertension model. Am J Physiol Heart Circ Physiol 2014;307:H1204–H1215.

Bleeker GB, Steendijk P, Holman ER, Yu C-M, Breithardt OA, Kaandorp TA, Schalij MJ, van der Wall EE, Nihoyannopoulos P, Bax JJ. Assessing right ventricular function: The role of echocardiography and complementary technologies. Heart 2006;92(Suppl 1):i19–i26.

Cameli M, Righini FM, Lisi M, Mondillo S. Right ventricular strain as a novel approach to analyze right ventricular performance in patients with heart failure. Heart Fail Rev 2014;19:603–610.

Chemla D, Castelain V, Zhu K, Papelier Y, Creuzé N, Hoette S, Parent F, Simonneau G, Humbert M, Herve P. Estimating right ventricular stroke work and the pulsatile work fraction in pulmonary hypertension. Chest 2013;143:1343–1350.

Chesler NC, Roldan A, Vanderpool RR, Naeije R. How to measure pulmonary vascular and right ventricular function. Conf Proc IEEE Eng Med Biol Soc 2009;2009:177–180.

Claessen G, La Gerche A, Voigt J-U, Dymarkowski S, Schnell F, Petit T, Willems R, Claus P, Delcroix M, Heidbuchel H. Accuracy of echocardiography to evaluate pulmonary vascular and rv function during exercise. JACC Cardiovasc Imaging 2016;9:532–543.

Currie PJ, Seward JB, Chan K-L, Fyfe DA, Hagler DJ, Mair DD, Reeder GS, Nishimura RA, Tajik AJ. Continuous wave Doppler determination of right ventricular pressure: A simultaneous Doppler-catheterization study in 127 patients. J Am Coll Cardiol 1985;6:750–756.

Dandel M, Krabatsch T, Falk V. Left ventricular vs. biventricular mechanical support: Decision making and strategies for avoidance of right heart failure after left ventricular assist device implantation. Int J Cardiol 2015;198:241–250.

Danton MHD, Greil GF, Byrne JG, Hsin M, Cohn L, Maier SE. Right ventricular volume measurement by conductance catheter. Am J Physiol Heart Circ Physiol 2003;285:H1774–H1785.

Dell'italia LJ, Walsh RA. Application of a time varying elastance model to right ventricular performance in man. Cardiovasc Res 1988;22:864–874.

Di Maria MV, Burkett DA, Younoszai AK, Landeck BF, Mertens L, Ivy DD, Friedberg MK, Hunter KS. Echocardiographic estimation of right ventricular stroke work in children with pulmonary arterial hypertension: Comparison with invasive measurements. J Am Soc Echocardiogr 2015;28:1350–1357.

Ensing G, Seward J, Darragh R, Caldwell R. Feasibility of generating hemodynamic pressure curves from noninvasive Doppler echocardiographic signals. J Am Coll Cardiol 1994;23:434–442.

Gorcsan J, Murali S, Counihan PJ, Mandarino WA, Kormos RL. Right ventricular performance and contractile reserve in patients with severe heart failure. Assessment by pressure-area relations and association with outcome. Circulation 1996;94:3190–3197.

Guihaire J, Haddad F, Boulate D, Decante B, Denault AY, Wu J, Hervé P, Humbert M, Dartevelle P, Verhoye J-P, Mercier O, Fadel E. Non-invasive indices of right ventricular function are markers of ventricular-arterial coupling rather than ventricular contractility: Insights from a porcine model of chronic pressure overload. Eur Heart J Cardiovasc Imaging 2013;14:1140–1149.

Haddad F, Hunt SA, Rosenthal DN, Murphy DJ. Right Ventricular function in cardiovascular disease, part I: Anatomy, physiology, aging, and functional assessment of the right ventricle. Circulation 2008;117:1436–1448.

Kass DA, Yamazaki T, Burkhoff D, Maughan WL, Sagawa K. Determination of left ventricular end-systolic pressure-volume relationships by the conductance (volume) catheter technique. Circulation 1986;73:586–595.

Kuehne T. Magnetic resonance imaging analysis of right ventricular pressure-volume loops: *In vivo* validation and clinical application in patients with pulmonary hypertension. Circulation 2004;110:2010–2016.

Lang RM, Badano LP, Mor-Avi V, Afilalo J, Armstrong A, Ernande L, Flachskampf FA, Foster E, Goldstein SA, Kuznetsova T, Lancellotti P, Muraru D, Picard MH, Rietzschel ER, Rudski L, Spencer KT, Tsang W, Voigt J-U. Recommendations for cardiac chamber quantification by echocardiography in adults: An update from the American Society of Echocardiography and the European Association of Cardiovascular Imaging. J Am Soc Echocardiogr 2015;28:1–39.

Lang RM, Badano LP, Tsang W, Adams DH, Agricola E, Buck T, Faletra FF, Franke A, Hung J, de Isla LP, Kamp O, Kasprzak JD, Lancellotti P, Marwick TH, McCulloch ML, Monaghan MJ, Nihoyannopoulos P, Pandian NG, Pellikka PA, Pepi M, Roberson DA, Shernan SK, Shirali GS, Sugeng L, Cate FJT, Vannan MA, Zamorano JL, Zoghbi WA. EAE/ASE Recommendations for image acquisition and display using three-dimensional echocardiography. J Am Soc Echocardiogr 2012;25:3–46.

Ling LF, Obuchowski NA, Rodriguez L, Popovic Z, Kwon D, Marwick TH. Accuracy and interobserver concordance of

echocardiographic assessment of right ventricular size and systolic function: A quality control exercise. J Am Soc Echocardiogr 2012; 25:709–713.

McKay RG, Spears JR, Aroesty JM, Baim DS, Royal HD, Heller GV, Lincoln W, Salo RW, Braunwald E, Grossman W. Instantaneous measurement of left and right ventricular stroke volume and pressure-volume relationships with an impedance catheter. Circulation 1984;69:703–710.

Medvedofsky D, Addetia K, Patel AR, Sedlmeier A, Baumann R, Mor-Avi V, Lang RM. Novel approach to three-dimensional echocardiographic quantification of right ventricular volumes and function from focused views. J Am Soc Echocardiogr 2015;28:1222–1231.

Mohammed SF, Hussain I, AbouEzzeddine OF, Takahama H, Kwon SH, Forfia P, Roger VL, Redfield MM. Right Ventricular function in heart failure with preserved ejection fraction: A community-based study. Circulation 2014;130:2310–2320.

Nagueh SF, Smiseth OA, Appleton CP, Byrd BF, Dokainish H, Edvardsen T, Flachskampf FA, Gillebert TC, Klein AL, Lancellotti P, Marino P, Oh JK, Popescu BA, Waggoner AD. Recommendations for the evaluation of left ventricular diastolic function by echocardiography: An update from the American Society of Echocardiography and the European Association of Cardiovascular Imaging. J Am Soc Echocardiogr 2016;29:277–314.

Rudski LG, Lai WW, Afilalo J, Hua L, Handschumacher MD, Chandrasekaran K, Solomon SD, Louie EK, Schiller NB. Guidelines for the echocardiographic assessment of the right heart in adults: A report from the American Society of Echocardiography. J Am Soc Echocardiogr 2010;23:685–713.

Ryo K, Goda A, Onishi T, Delgado-Montero A, Tayal B, Champion HC, Simon MA, Mathier MA, Gladwin MT, Gorcsan J. Characterization of right ventricular remodeling in pulmonary hypertension associated with patient outcomes by 3-dimensional wall motion tracking echocardiography. Circ Cardiovasc Imaging 2015;8:e003176.

Shah SJ, Katz DH, Selvaraj S, Burke MA, Yancy CW, Gheorghiade M, Bonow RO, Huang C-C, Deo RC. Phenomapping for novel classification of heart failure with preserved ejection fraction. Circulation 2015;131:269–279.

Szwarc RS, Ball HA. Simultaneous LV and RV volumes by conductance catheter: Effects of lung insufflation on parallel conductance. Am J Physiol 1998;275:H653–H661.

Szwarc RS, Laurent D, Allegrini PR, Ball HA. Conductance catheter measurement of left ventricular volume: Evidence for nonlinearity within cardiac cycle. Am J Physiol 1995;268:H1490–H1498.

Vachiéry J-L, Adir Y, Barberà JA, Champion H, Coghlan JG, Cottin V, De Marco T, Galiè N, Ghio S, Gibbs JSR, Martinez F, Semigran M, Simonneau G, Wells A, Seeger W. Pulmonary hypertension due to left heart diseases. J Am Coll Cardiol 2013;62:D100–D108.

Wright LM, Dwyer N, Celermajer D, Kritharides L, Marwick TH. Follow-up of pulmonary hypertension with echocardiography. JACC Cardiovasc Imaging 2016;9:733–746.